HHS Public Access

Author manuscript

Cancer Cell. Author manuscript; available in PMC 2015 July 07.

Published in final edited form as:

Cancer Cell. 2014 March 17; 25(3): 393–405. doi:10.1016/j.ccr.2014.02.004.

Genome Sequencing of SHH Medulloblastoma Predicts Genotype-Related Response to Smoothened Inhibition

A full list of authors and affiliations appears at the end of the article.

Summary

Smoothened (SMO) inhibitors recently entered clinical trials for sonic-hedgehog-driven medulloblastoma (SHH-MB). Clinical response is highly variable. To understand the mechanism(s) of primary resistance and identify pathways cooperating with aberrant SHH signaling, we sequenced and profiled a large cohort of SHH-MBs (n = 133). SHH pathway mutations involved *PTCH1* (across all age groups), *SUFU* (infants, including germline), and *SMO* (adults). Children >3 years old harbored an excess of downstream *MYCN* and *GLI2* amplifications and frequent *TP53* mutations, often in the germline, all of which were rare in infants and adults. Functional assays in different SHH-MB xenograft models demonstrated that SHH-MBs harboring a *PTCH1* mutation were responsive to SMO inhibition, whereas tumors harboring an *SUFU* mutation or *MYCN* amplification were primarily resistant.

Introduction

Medulloblastoma (MB) comprises a collection of clinically and molecularly distinct tumor subgroups that arise either in the cerebellum or brainstem (Grammel et al., 2012; Louis et al., 2007; Taylor et al., 2012). In children, they comprise the most frequent embryonal brain tumor, whereas in adults the disease is relatively rare, accounting for less than 1% of all intracranial malignancies (Louis et al., 2007). Current therapy regimens including surgery, cranio-spinal radiotherapy, and chemotherapy, may cure 70%–80% of patients with MB. Most survivors, however, suffer from long-term sequelae because of the intensive treatment, demonstrating that less toxic treatments are urgently needed. Molecular analyses have shown that there are four major MB subgroups (WNT, Sonic Hedgehog [SHH], Group 3, and Group 4; Taylor et al., 2012). They are highly distinct in tumor cell histology and biology, and in addition show divergent clinical phenotypes such as patient demographics, tumor dissemination, and patient outcome (Kool et al., 2012; Northcott et al., 2012a; Taylor et al., 2012). Recent studies, largely focusing on pediatric MB, have utilized next-generation sequencing technologies to map the genomic landscape of MB and to identify novel driver mutations in each molecular subgroup (Jones et al., 2012; Northcott et al., 2012a, 2012b;

Correspondence to: Marcel Kool, m.kool@dkfz.de.

[44]These authors contributed equally to this work and are co-senior authors

Accession Numbers: The Gene Expression Omnibus accession numbers for the complete CpG methylation values are GSE49576 and GSE49377; for the complete gene expression values, the number is GSE49243. The European Genome-phenome Archive accession number for the sequencing data is EGAS00001000607.

Supplemental Information: Supplemental Information includes Supplemental Experimental Procedures, three figures, and four tables and can be found with this article online at http://dx.doi.org/10.1016/j.ccr.2014.02.004.

Parsons et al., 2011; Pugh et al., 2012; Rausch et al., 2012; Robinson et al., 2012). Due to the infrequent occurrence of this disease in adulthood, little is known about the biology and genetics of MB in adults. This also explains why there are few prospective phase III trials for this age group. Most centers treat adult patients with MB either using glioblastoma protocols (which are largely ineffective) or, alternatively, using pediatric MB protocols, although toxicity profiles differ greatly between children and adults, leading to dose-limiting toxicity in a high proportion of adults treated on pediatric protocols (Brandes et al., 2009; Padovani et al., 2007; Spreafico et al., 2005).

Targeted therapy as an alternative treatment option for patients with MB is especially interesting for SHH-MBs. SHH pathway antagonists, primarily those inhibiting at the level of smoothened (SMO), are currently a major area of interest in the pharmaceutical industry because they can potentially be applied in multiple cancers with activated SHH signaling (Lin and Matsui, 2012). Some of these drugs are already in clinical trials for MB (Low and de Sauvage, 2010; Ng and Curran, 2011). SHH-MBs with alterations in downstream SHH pathway genes, however, such as *SUFU*, *GLI2*, or *MYCN*, may demonstrate primary resistance to SMO inhibition (Lee et al., 2007). Furthermore, as has been shown in both humans and mice, tumors may also rapidly acquire secondary resistance to treatment (Dijkgraaf et al., 2011; Rudin et al., 2009; Yauch et al., 2009), suggesting that such inhibitors might be ineffective as a curative option when administered as monotherapy. SHH-MBs present the most common subgroup in infants (≤3 years old) and adults (≥18 years old), whereas in children (4–17 years old) other subgroups are more prevalent (Kool et al., 2012). Transcriptome analyses and whole genome sequencing have already shown that SHH-MBs are quite heterogeneous (Northcott et al., 2011a; Rausch et al., 2012). Childhood SHH-MBs, for instance, are genetically distinct from those in infants, because they frequently harbor *TP53* mutations and as a result of chromothripsis, their genomes are often dramatically rearranged (Rausch et al., 2012). To preselect patients who might qualify for clinical trials using SMO antagonists or future combination therapies, a better understanding of the biology of SHH-MBs across different age groups is required. We have therefore sequenced the genomes of 133 cases of SHH-MB, including 50 adult and 83 pediatric cases. In addition, we analyzed the tumors for DNA methylation and gene expression.

Results

SHH-MBs in Infants, Children, and Adults Are Genomically Distinct

Unsupervised *k*-means consensus cluster analysis of DNA methylation data (n = 129) identified two major clusters, mainly separating infant from childhood and adult SHH-MB tumors (Figure 1A, left panel). Unsupervised cluster analysis of gene expression data (n = 103) showed similar results, with the infant cases again being the most distinct (Figure 1A, right panel). GISTIC2 analysis of somatic copy number aberrations in all SHH-MB cases (n = 266) reported by MAGIC (Northcott et al., 2012b), however, showed that childhood SHH-MBs are very different from both infant and adult SHH-MBs (Figure 1B). Childhood SHH-MBs typically show much greater genomic instability and are characterized by frequent amplifications of oncogenes including *GLI2*, *MYCN*, and *PPM1D*, most likely due to underlying chromosome shattering (chromothripsis; Rausch et al., 2012).

Next-Generation Sequencing of SHH-MB

To determine the mutational landscape of SHH-MBs across age groups, we sequenced a large series of SHH-MB tumors from infants (≤3 years old; n = 50), children (4–17 years old; n = 33), and adults (≥18 years old; n =50; Table 1; Table S1 available online). In the discovery cohort of 67 SHH-MBs, analyzed by whole genome or whole exome sequencing, we identified 1,090 nonsynonymous somatic single nucleotide variants (SNVs) and 155 small insertions or deletions (indels), 89 of which introduced translational frameshifts and 9 affected splice sites. In total, 1,054 genes were found to be somatically mutated in this discovery cohort, including 78 with alterations in more than one tumor. In the two replication cohorts (43 pediatric and 23 adults), we identified another 666 nonsynonymous SNVs and 76 indels. For the combined 133 SHH-MBs, we found mutations in 1,156 genes, 215 of which were recurrently altered. All coding somatic SNVs/indels identified are listed in Table S2.

As previously reported (Jones et al., 2012), pediatric SHH-MBs harbored very few nonsynonymous SNVs (infants, 0–13, median 3.0; children [*TP53* wild-type], 1–26, median 9.5; Table S2; Figures 2A and 2B). Exceptions were the eight *TP53* mutated tumors in children, in this discovery cohort all between 9.5 and 14 years old, which harbored on average many more mutations (7–29, median 19.5). WGS data showed that adult SHH-MBs also contained many more nonsynonymous SNVs (9–48, median 25.0), in line with other adult solid tumors. The average number of small indels was also higher in adults (0–10, median 3.0) than in children (0–4, median 1.0) and infants (0–3, median 1.0). Interestingly, there was a much stronger correlation between somatic mutation rate and patient age, both genome-wide ($r^2 = 0.58$, $p = 1.6 \times 10^{-9}$, Pearson's product moment correlation), and for coding mutations ($r^2 = 0.62$, $p = 2.2 \times 10^{-15}$), than previously reported across all MB subgroups (Figures 2A and 2B; Jones et al., 2012). Assessment of mutation classes revealed a predominance of cytosine to thymine (C > T) transitions in a CpG context (likely due to deamination of methylated cytosines), as expected for an age-related background mutation pattern (Figures 2C and 2D; Welch et al., 2012). Interestingly, the C > T fraction in the *TP53* mutated cases appeared to be much lower, with a relatively higher proportion of cytosine to adenosine (C > A) transitions. Whether this can be explained by the *TP53* mutation itself remains elusive.

Mutations in the SHH Pathway

Overall, we detected mutations in known SHH pathway genes (116/133 cases; 87%), further substantiating the tumor-driving role of the SHH pathway in this medulloblastoma subgroup (Table S3). As expected, among the most frequently mutated genes were *PTCH1* (60 cases), *SMO* (19 cases), and *SUFU* (10 cases), all mutually exclusive (Figure 3A; Figures S1A–S1C). In addition, we found two *PTCH1* and six *SUFU* mutations in the germlines of eight pediatric patients, including two twin brothers with an identical small indel in *SUFU* (Table S3). The second replication cohort (for which germline controls were unavailable) contained another two cases from twin brothers both with the same inactivating *SUFU* mutation, strongly suggesting that this was also a germline event. For all other samples in this replication cohort, it remains unknown whether any of the identified *PTCH1* or *SUFU* mutations were germline events. Interestingly, while *PTCH1* mutations were found at

roughly equal frequency in infants (42.0%), children (36.4%), and adults (54.0%), *SMO* mutations were highly enriched in adult patients (15/19 mutations; $p = 1.8 \times 10^{-4}$), while *SUFU* mutations were almost exclusively found in infants ≤3 years old (16/18 mutations; $p = 8.4 \times 10^{-6}$). Mutations in *SMO* and *SUFU* were absent or extremely rare in children (4–17 years old; Figures 3A and 3B). Instead, they frequently harbored *TP53* mutations (16/33 children; $p = 1.2 \times 10^{-11}$), all found in children between 8 and 17 years old. The *TP53* mutations were mutually exclusive with *PTCH1* mutations but often co-occurred with amplifications of *GLI2* ($p = 2.5 \times 10^{-6}$) and *MYCN* ($p = 2.8 \times 10^{-8}$), three events that were rare in infants, young children, and adults (Figures 3A and 3B). In addition, we identified four cases, including three children with a *TP53* mutation, with an amplification of the *SHH* gene. These results show that activating mutations in the SHH pathway are detectable in almost all SHH-MBs, but the type of mutation and targeted genes are largely variable in the different age groups (Figure 3C).

Large Cell/Anaplastic Histology and 17p Loss Are Strongly Associated with TP53 Mutated SHH-MBs

Losses of 9q, 10q, and/or 17p are the most common copy number aberrations associated with SHH-MBs (Kool et al., 2012). All three were most frequent in childhood cases, with 17p loss highly enriched in *TP53* mutant cases (14/17 had 17p loss; $p = 7.8 \times 10^{-8}$; Figures 3A and 3B). Histology was also unequally distributed between the three age groups, with most large cell/anaplastic (LCA) cases found in childhood (15/21; $p = 4.1 \times 10^{-9}$). Thirteen of these 15 had a *TP53* mutation. Nodular/desmoplastic MB variants were most prevalent in infant cases. Moreover, all four MBs with extensive nodularity (MBEN) were found in infants (Figures 3A and 3B). In contrast to a recent report (Brugières et al., 2012), which was, however, reporting on a larger number of MBEN MBs, only 1/4 MBEN cases in our series had an *SUFU* mutation, while two harbored a *PTCH1*, and one displayed an *SMO* mutation (Figure 3A).

TERT Promoter Mutations Are Highly Recurrent in Adult SHH-MBs

Recently, several groups have reported that *TERT* promoter mutations that drive telomerase activity are frequently found in various cancers, including medulloblastoma, of mainly adult patients (Killela et al., 2013; Koelsche et al., 2013; Remke et al., 2013). Two mutually exclusive hotspot mutations in the promoter region have been reported: C228T and the less frequent C250T. Using our WGS data and data from the replication cohort in which the *TERT* promoter region was analyzed by PCR and Sanger sequencing (Remke et al., 2013), we found that indeed these mutations almost exclusively and with high frequency occur in adult SHH-MBs (Table S1). Strikingly, almost all adult patients for which we had data available had a somatic *TERT* promoter mutation (43/44, 98%; 40 had the C228T mutation and 3 had the C250T mutation). In contrast, in infants and children, only 3/24 (13%) and 3/14 (21%) SHH-MBs, respectively, had a *TERT* mutation (five C228T and one C250T).

DDX3X and Chromatin Modifiers Are Frequently Mutated in Adult SHH-MBs

Other genes previously reported as being recurrently mutated in pediatric SHH-MBs (*MLL2*, *BCOR*, and *LDB1*) were also found in adult SHH-MBs (Figures 4A–4C). Interestingly,

however, we identified several recurrent mutations in adult SHH-MBs that were completely absent or very rare in pediatric SHH-MBs, including *BRPF1*, *KIAA0182*, *TCF4*, *CREBBP*, *NEB*, *LRP1B*, *PIK3CA*, *FBXW7*, *KDM3B*, *XPO1*, *PRKAR1A*, and *PDE4D* (Figures 4A-4C; Figures S1D-S1I). Another striking example is the gene encoding the RNA helicase DDX3X, which was mutated in 27 adult SHH-MBs (54%) and only 6 pediatric MBs (7.2%, $p = 4.5 \times 10^{-9}$). *DDX3X* was among the new genes identified in recent sequencing studies of pediatric MB (Jones et al., 2012; Pugh et al., 2012; Robinson et al., 2012). Notably, whereas mutations were found in 50% of WNT-MBs in children (Northcott et al., 2012a), few *DDX3X* mutations were seen in SHH-MBs in these studies (Pugh et al., 2012; Robinson et al., 2012). All identified mutations affected one of the two helicase domains with no difference in their distribution between WNT- and SHH-MBs (Figure S1D). Interestingly, mutations affecting the SWI-SNF complex, also mainly found in the WNT-MBs in children (Jones et al., 2012; Northcott et al., 2012a; Pugh et al., 2012; Robinson et al., 2012), were also frequently seen in adult SHH-MBs.

Pathway analyses, performed separately for the three age groups, showed marked differences in altered processes. In infant cases, developmental processes and DNA/histone methylation are prominently affected. Both in children and in adults, chromatin organization is also affected, but especially in adults many more chromatin modifiers and/or transcription regulators were additionally altered, as well as different and larger gene sets involved in brain development (Figure S2 and Table S4). Remarkably, most of the mutations in chromatin modifiers in adults were found to be mutually exclusive (Figure 4D). Interestingly, some of these mutations in chromatin modifiers were more closely associated with *SMO* mutations, like the ones in *BRPF1/3*, while mutations in *CREBBP* or *KDM3B* were more often found in *PTCH1*-mutated tumors.

PI3K/AKT Signaling Activated in Adult SHH-MB Associates with Poor Outcome

As we identified recurrent mutations affecting the PI3K/AKT/mTOR-pathway in SHH-MBs (*PIK3CA*, *PTEN*, and *PIK3C2G* are all mutated in >5% of SHH-MBs; Figures 4A–4C), which could lead to GLI activation independent of SMO (Wang et al., 2012), targeting this pathway could be an option for combination therapies. To investigate which SHH patients would be most suitable for targeting PI3K/AKT/mTOR-signaling, we examined activation of the pathway in a large series of SHH-MBs (n = 155) by immunohistochemistry using antibodies for p-AKT and p-S6. p-AKT and p-S6 positivity were each detected in 17% of cases, with 12% positive for both (Figures 5A–5F). Surprisingly, the vast majority of positive cases were tumors from adult patients, with 31% and 30% of the adult SHH-MBs staining positive for p-AKT or p-S6, respectively. Moreover, survival analysis showed that both p-AKT and p-S6 positivity were strongly associated with a poor outcome in adult patients with SHH-MB (Figure 5G). Other factors shown to be associated with a poor outcome in SHH-MB patients, like *MYCN or GLI2* amplification, LCA histology or metastasis at diagnosis, are all exceptionally rare in adult SHH-MB patients (Figures 1C and 3A; Kool et al., 2012), and could therefore not explain the poor outcome of these p-AKT/p-S6-positive subgroup of patients. Our results suggest that adult patients with SHH-MB may be the best group to benefit from combination therapies of SMO inhibitors with PI3K/AKT/mTOR inhibition.

SHH Medulloblastomas with Mutations Downstream of SMO Are Resistant to LDE-225

Assuming a linear pathway, we anticipate that patients with mutations in the SHH pathway downstream of SMO (e.g., *SUFU*, *GLI2*, and *MYCN*) show primary resistance to targeted SMO inhibition. To test this hypothesis, we used xenografts from three SHH-associated MBs (DMB-012, RCMB-018, and RCMB-025; Yeh-Nayre et al., 2012). These xenografts were generated by stereotaxic orthotopic xenotransplantation of cells immediately after surgical resection, maintained by serial intracranial transplantation, and harvested only for use in short-term experiments, allowing them to maintain the characteristics of the original tumors (Shu et al., 2008; Zhao et al., 2012). WES showed that each xenograft harbored a different alteration in the SHH pathway (Figure 6A). Cells from each xenograft line were treated in vitro with NVP-LDE225, an SMO inhibitor that is currently being applied in phase III clinical trials for relapsed childhood and adult SHH-MB (Geoerger et al., 2012). Proliferation was measured based on incorporation of tritiated thymidine. Treatment with LDE225 significantly inhibited the proliferation of DMB-012 cells (*PTCH1* mutant), but did not affect the proliferation of RCMB-018 (*MYCN* amplification) or RCMB-025 cells (*SUFU* deletion; Figures 6B–6D). Preclinical testing in vivo also demonstrated a strong inhibition of tumor growth by LDE225 in DMB-012 (Figure 6E), but not RCMB-018 (Figure 6F and Figure S3), confirming the in vitro data. Survival analyses indeed show that mice with DMB-012 tumors live longer when treated with LDE-225 (Figure 6G), but mice with RCMB-018 tumors do not (Figure 6H). Finally, we have tested whether RCMB-018 cells, resistant to LDE-225, are responsive to arsenic trioxide (ATO) targeting cells at the level of GLI (Beauchamp et al., 2011). Figure 6I illustrates that RCMB-018 cells are responsive to ATO. At concentrations of 5–10 μM, cells are markedly inhibited in growth. Our data show that classification as an SHH-MB using a five-gene expression signature currently being applied in clinical trials is not sufficient as a predictive biomarker for response to SMO antagonists, because all SHH-MBs are detected by this signature, regardless of their underlying genetic makeup (Amakye et al., 2012).

Discussion

Herein we have shown that genetic hits in SHH-MBs are very heterogeneous. Tumors in infants, children, and adults strongly differ in transcriptome, methylome, and copy-number aberrations as well as in number and type of mutations they contain. Hereditary predisposition syndromes involving germline mutations of *SUFU* (or rarely *PTCH1*; Gorlin syndrome) are highly prevalent in infant (0–3 years old) SHH-MBs, while germline *TP53* mutations (Li-Fraumeni syndrome) are common in older children (>3 years old), especially in children between 8 and 17 years old. Strikingly, almost all adults harbored somatic mutations in the *TERT* promoter, whereas they were much less common in pediatric patients. Our data show that three groups of SHH-MBs should be considered: young children with mostly *PTCH1* or *SUFU* mutations, older children with frequent germline *TP53* mutations and chromothripsis-associated amplifications of SHH pathway genes, and adults harboring mostly *PTCH1* and *SMO* mutations (Figure 3C). Recent data showing that SHH-MBs can arise from different precursor cells in the cerebellum or brainstem (Grammel et al., 2012) suggest that infant SHH-MBs may have a different cellular origin or hit the

same progenitor cell at a different stage of differentiation than childhood or adult SHH-MBs (which were more similar at the transcriptome/methylome levels).

Most importantly, our results show that patients with different underlying SHH mutations should be stratified accordingly. We have demonstrated that targeting the SHH pathway in SHH-MB using SMO antagonists will most likely give the best results in adult patients. A vast majority (82%) of adult patients harbor tumors with mutations in either *PTCH1* or *SMO*, rendering them likely responsive to these drugs. In contrast, infant (36%) and childhood (45%) SHH-MBs frequently have mutations downstream of SMO, which makes these tumors intrinsically resistant to drugs targeting SMO. Indeed, SHH-MB xenografts harboring these downstream mutations did not respond to SMO antagonists. The impact of bone developmental toxicity may additionally limit the use of SMO inhibitors in infants (Kimura et al., 2008).

Furthermore, our results strongly suggest that each patient with a SHH-MB, but especially those between 4 and 17 years of age with LCA histology, should be tested for germline *TP53* mutations. Currently, these patients with Li-Fraumeni syndrome (LFS)-MB are often not recognized and therefore treated with standard protocols, including ionizing radiotherapy and alkylating chemotherapy. Moreover, as almost all patients with germline *TP53* mutations have tumors with LCA histology, they are often stratified as high risk and will therefore get even higher doses of radiotherapy and chemotherapy. It seems that these patients are often cured of their MB, but frequently die of secondary malignancies induced by previous radio-chemotherapy. This may partly explain why *TP53* mutations in SHH-MBs are associated with a particularly poor outcome (Zhukova et al., 2013), and is also in line with the finding that *MYCN* amplification in SHH-MBs is associated with an inferior prognosis (Kool et al., 2012; Korshunov et al., 2012; Ryan et al., 2012). We therefore strongly suggest that separate LFS-MB trials should be developed using chemotherapy-only protocols and excluding alkylating drugs.

We further strongly advocate that the next generation of SMO inhibitor trials should be based on underlying tumor genetics because many patients with SHH-MB will not respond to these inhibitors. Alternative treatment options could include arsenic trioxide (ATO) targeting GLI transcription factors by degrading the protein (Figure 7; Kim et al., 2010, 2013). ATO and the antifungal agent itraconazole (which acts on SMO) have also been suggested in preclinical experiments for use in SHH-MBs that become resistant after treatment with SMO antagonists (Kim et al., 2013) or in combination with SMO inhibitors upfront knowing that *GLI2* amplifications comprise a common mechanism of secondary resistance to SMO inhibition in preclinical models (Buonamici et al., 2010; Dijkgraaf et al., 2011). Other options for combination therapies to avoid or delay the development of resistance include drugs targeting PI3K/AKT/mTOR- or PKA-signaling pathways (Figure 7), both mutated in a subset of patients with SHH and both also leading to GLI activation (Metcalfe et al., 2013; Milenkovic and Scott, 2010; Wang et al., 2012), or epigenetic drugs.

Experimental Procedures

Patient Samples

Patient materials were collected after receiving informed consent according to International Cancer Genome Consortium guidelines (http://www.icgc.org) and as approved by the institutional review board of contributing centers. DNA derived from SHH-MBs and matched normal blood from 45 patients was subjected to whole genome sequencing (WGS) using Illumina technologies. Two additional tumor-normal pairs were sequenced by whole exome sequencing (WES). WGS data for 13/45 and WES data for another 20 pediatric tumor-normal pairs were previously reported (Jones et al., 2012; Pugh et al., 2012). All patients in this discovery cohort (n = 67) were confirmed to have a MB of the SHH subtype by either gene expression profiling, DNA methylation, or immunohistochemistry (SFRP1 Northcott et al., 2011b and GAB1 Ellison et al., 2011). In addition, we used data from 12 pediatric SHH-MB tumor-normal pairs that were sequenced for 2,734 genes as part of a previously reported replication cohort (Jones et al., 2012). Finally, a set of 400 genes, including those identified as recurrently mutated in SHH-MBs in our discovery cohort, was investigated in another independent set of pediatric (31) and adult (23) SHH-MBs, for which only tumor DNA was available. In total, sequencing data for 133 (83 pediatric and 50 adult) SHH-MBs are presented in this study. Patient details are listed in Table S1.

Animals

Immunocompromised (NOD-scid IL2Rgammanull or NSG) mice used for transplantation were purchased from Jackson Labs. Mice were maintained in the Animal Facility at Sanford-Burnham. All experiments were performed in accordance with national guidelines and regulations, and with the approval of the animal care and use committee at Sanford-Burnham.

The experimental procedures used in this study are described in more detail in the Supplemental Experimental Procedures.

Authors

Marcel Kool[1], David T.W. Jones[1], Natalie Jäger[2], Paul A. Northcott[1], Trevor J. Pugh[3], Volker Hovestadt[4], Rosario M. Piro[2], L. Adriana Esparza[5], Shirley L. Markant[5], Marc Remke[6], Till Milde[7], Franck Bourdeaut[8,9], Marina Ryzhova[10], Dominik Sturm[1], Elke Pfaff[1], Sebastian Stark[1], Sonja Hutter[1], Huriye Şeker-Cin[1], Pascal Johann[1], Sebastian Bender[1], Christin Schmidt[1], Tobias Rausch[11], David Shih[6], Jüri Reimand[12], Laura Sieber[1], Andrea Wittmann[1], Linda Linke[1], Hendrik Witt[1,7], Ursula D. Weber[4], Marc Zapatka[4], Rainer König[2,13,14], Rameen Beroukhim[3,15,16], Guillaume Bergthold[3,15,17], Peter van Sluis[18], Richard Volckmann[18], Jan Koster[18], Rogier Versteeg[18], Sabine Schmidt[19], Stephan Wolf[19], Chris Lawerenz[20], Cynthia C. Bartholomae[21], Christof von Kalle[21], Andreas Unterberg[21], Christel Herold-Mende[21], Silvia Hofer[22], Andreas E. Kulozik[7], Andreas von Deimling[23,24], Wolfram Scheurlen[25], Jörg Felsberg[26], Guido Reifenberger[26], Martin Hasselblatt[27], John R. Crawford[28,29], Gerald A. Grant[30,31], Nada Jabado[32], Arie Perry[33], Cynthia Cowdrey[34], Sydney Croul[35], Gelareh Zadeh[35], Jan O.

Korbel[11], Francois Doz[8,36], Olivier Delattre[8,9], Gary D. Bader[12], Martin G. McCabe[37], V. Peter Collins[38], Mark W. Kieran[39], Yoon-Jae Cho[40], Scott L. Pomeroy[41], Olaf Witt[42], Benedikt Brors[2], Michael D. Taylor[6], Ulrich Schüller[43], Andrey Korshunov[1,23,24], Roland Eils[2], Robert J. Wechsler-Reya[5,44], Peter Lichter[4,44], and Stefan M. Pfister[1,7,44] **on behalf of the ICGC PedBrain Tumor Project**

Marcel Kool: m.kool@dkfz.de

Affiliations

[1]Division of Pediatric Neurooncology, German Cancer Research Center (DKFZ), 69121 Heidelberg, Germany [2]Division of Theoretical Bioinformatics, German Cancer Research Center (DKFZ), 69121 Heidelberg, Germany [3]Broad Institute of MIT and Harvard, Cambridge, MA 02141, USA [4]Division of Molecular Genetics, German Cancer Research Center (DKFZ), 69121 Heidelberg, Germany [5]Sanford-Burnham Medical Research Institute, La Jolla, CA 92037, USA [6]The Arthur and Sonia Labatt Brain Tumour Research Centre, Hospital for Sick Children, Toronto, ON M5G 1L7, Canada [7]Department of Pediatric Oncology, Hematology and Immunology, University Hospital Heidelberg, 69120 Heidelberg, Germany [8]Institut Curie, 75005 Paris, France [9]Institut Curie/INSERM U830, 75248 Paris, France [10]Department of Neuropathology, NN Burdenko Neurosurgical Institute, Moscow 125047, Russia [11]European Molecular Biology Laboratory (EMBL), 69117 Heidelberg, Germany [12]The Donnelly Centre, University of Toronto, Toronto, ON M5S 3E1, Canada [13]Integrated Research and Treatment Center, Center for Sepsis Control and Care, Jena University Hospital, 07747 Jena, Germany [14]Leibniz Institute for Natural Product Research and Infection Biology, Hans-Knöll-Institute (HKI), 07745 Jena, Germany [15]Department of Cancer Biology, Dana Farber Cancer Institute, Boston, MA 02215, USA [16]Department of Medicine, Brigham and Women's Hospital and Harvard Medical School, Boston, MA 02115, USA [17]UMR 8203, CNRS Vectorology and Anticancer Therapeutics, Gustave Roussy Cancer Institute, University Paris XI, 94805 Villejuif Cedex, France [18]Department of Oncogenomics, Academic Medical Center, Amsterdam 1105 AZ, the Netherlands [19]Genomics and Proteomics Core Facility, German Cancer Research Center (DKFZ), 69121 Heidelberg, Germany [20]Data Management Facility, German Cancer Research Center (DKFZ), 69121 Heidelberg, Germany [21]Division of Translational Oncology, German Cancer Research Center (DKFZ) and National Center for Tumor Diseases (NCT), 69121 Heidelberg, Germany [22]Department of Oncology, University Hospital Zürich, 8006 Zürich, Switzerland [23]Department of Neuropathology, University of Heidelberg, 69120 Heidelberg, Germany [24]Clinical Cooperation Unit Neuropathology, German Cancer Research Center (DKFZ), 69121 Heidelberg, Germany [25]Cnopf'sche Kinderklinik, Nürnberg Children's Hospital, 90419 Nuürnberg, Germany [26]Department of Neuropathology, Heinrich-Heine-University Düsseldorf, 40225 Düsseldorf, Germany [27]Institute for Neuropathology, University Hospital Münster, 48149 Münster, Germany [28]Departments of Pediatrics and Neurosciences, University of California San Diego, La Jolla, CA 92093 [29]Rady Children's Hospital, San Diego, CA 92123, USA [30]Division of Pediatric Hematology/

Oncology, Department of Pediatrics, Duke University Medical Center, Durham, NC 27710, USA [31]Department of Surgery, Duke University Medical Center, Durham, NC 27710, USA [32]Departments of Pediatrics and Human Genetics, McGill University Health Centre Research Institute, Montreal, QC H3H 1P3, Canada [33]Departments of Pathology and Laboratory Medicine, University of California, San Francisco, San Francisco, CA 94143, USA [34]Departments of Pathology and Neurological Surgery, Brain Tumor Research Center, University of California, San Francisco, San Francisco, CA 94143, USA [35]Department of Neuropathology, The Arthur and Sonia Labatt Brain Tumour Research Centre, Toronto, ON M5G 1L7, Canada [36]Université Paris Descartes, 75006 Paris, France [37]Manchester Academic Health Science Centre, Manchester M13 9NT, UK [38]Department of Pathology, University of Cambridge, Cambridge CB2 1QP, UK [39]Pediatric Medical Neuro-Oncology, Dana-Farber Cancer Institute and Boston Children's Hospital, Boston, MA 02215, USA [40]Department of Neurology and Neurosurgery, Stanford University School of Medicine, Stanford, CA 94305, USA [41]Boston Children's Hospital and Harvard Medical School, Boston, MA 02115, USA [42]CCU Pediatric Oncology, German Cancer Research Center (DKFZ), 69121 Heidelberg, Germany [43]Center for Neuropathology and Prion Research, Ludwig-Maximilians-Universität, 81377 München, Germany

Acknowledgments

For technical support and expertise, we thank the people from the DKFZ Genomics and Proteomics Core Facility, Malaika Knopf from the NCT Heidelberg, and GATC Biotech AG for sequencing services. This work was principally supported by the PedBrain Tumor Project (http://www.pedbraintumor.org) contributing to the International Cancer Genome Consortium, funded by German Cancer Aid (109252) and by the German Federal Ministry of Education and Research (Bundesministerium für Bildung und Forschung, grant numbers 01KU1201A, MedSys 0315416C, and NGFNplus 01GS0883). Additional support came from the Dutch Cancer Foundations KWF (2010-4713) and KIKA (to M.K.), and the Brain Tumor Charity (to V.P.C.). G.R. received a research grant from Roche and honoraria for advisory boards from Merck Serono and Roche. R.B. and O.W. are consultants for and received grant funding from Novartis.

References

Amakye DD, Robinson D, Rose K, Cho Y, Ligon K, Sharp T, Haider A, Bandaru R, Ando Y, Geoerger B, et al. Abstract 4818: The predictive value of a 5-gene signature as a patient pre-selection tool in medulloblastoma for Hedgehog pathway inhibitor therapy. Cancer Res. 2012; 72 http://dx.doi.org/10.1158/1538-7445.AM2012-4818.

Beauchamp EM, Ringer L, Bulut G, Sajwan KP, Hall MD, Lee YC, Peaceman D, Ozdemirli M, Rodriguez O, Macdonald TJ, et al. Arsenic trioxide inhibits human cancer cell growth and tumor development in mice by blocking Hedgehog/GLI pathway. J Clin Invest. 2011; 121:148–160. [PubMed: 21183792]

Brandes AA, Franceschi E, Tosoni A, Reni M, Gatta G, Vecht C, Kortmann RD. Adult neuroectodermal tumors of posterior fossa (medulloblastoma) and of supratentorial sites (stPNET). Crit Rev Oncol Hematol. 2009; 71:165–179. [PubMed: 19303318]

Brugières L, Remenieras A, Pierron G, Varlet P, Forget S, Byrde V, Bombled J, Puget S, Caron O, Dufour C, et al. High frequency of germline SUFU mutations in children with desmoplastic/nodular medulloblastoma younger than 3 years of age. J Clin Oncol. 2012; 30:2087–2093. [PubMed: 22508808]

Buonamici S, Williams J, Morrissey M, Wang A, Guo R, Vattay A, Hsiao K, Yuan J, Green J, Ospina B, et al. Interfering with resistance to smoothened antagonists by inhibition of the PI3K pathway in medulloblastoma. Sci Transl Med. 2010; 2:51ra70.

Dijkgraaf GJ, Alicke B, Weinmann L, Januario T, West K, Modrusan Z, Burdick D, Goldsmith R, Robarge K, Sutherlin D, et al. Small molecule inhibition of GDC-0449 refractory smoothened mutants and downstream mechanisms of drug resistance. Cancer Res. 2011; 71:435–444. [PubMed: 21123452]

Ellison DW, Dalton J, Kocak M, Nicholson SL, Fraga C, Neale G, Kenney AM, Brat DJ, Perry A, Yong WH, et al. Medulloblastoma: clinicopathological correlates of SHH, WNT, and non-SHH/WNT molecular subgroups. Acta Neuropathol. 2011; 121:381–396. [PubMed: 21267586]

Geoerger B, Aerts I, Casanova M, Chisholm JC, Hargrave D, Leary S, Ashley DM, Bouffet E, MacDonald TJ, Hurh E, et al. A phase I/II study of LDE225, a smoothened (Smo) antagonist, in pediatric patients with recurrent medulloblastoma (MB) or other solid tumors. J Clin Oncol. 2012; 30:9519.

Grammel D, Warmuth-Metz M, von Bueren AO, Kool M, Pietsch T, Kretzschmar HA, Rowitch DH, Rutkowski S, Pfister SM, Schüller U. Sonic hedgehog-associated medulloblastoma arising from the cochlear nuclei of the brainstem. Acta Neuropathol. 2012; 123:601–614. [PubMed: 22349907]

Jones DT, Jäger N, Kool M, Zichner T, Hutter B, Sultan M, Cho YJ, Pugh TJ, Hovestadt V, Stütz AM, et al. Dissecting the genomic complexity underlying medulloblastoma. Nature. 2012; 488:100–105. [PubMed: 22832583]

Killela PJ, Reitman ZJ, Jiao Y, Bettegowda C, Agrawal N, Diaz LA Jr, Friedman AH, Friedman H, Gallia GL, Giovanella BC, et al. TERT promoter mutations occur frequently in gliomas and a subset of tumors derived from cells with low rates of self-renewal. Proc Natl Acad Sci USA. 2013; 110:6021–6026. [PubMed: 23530248]

Kim J, Tang JY, Gong R, Kim J, Lee JJ, Clemons KV, Chong CR, Chang KS, Fereshteh M, Gardner D, et al. Itraconazole, a commonly used antifungal that inhibits Hedgehog pathway activity and cancer growth. Cancer Cell. 2010; 17:388–399. [PubMed: 20385363]

Kim J, Aftab BT, Tang JY, Kim D, Lee AH, Rezaee M, Kim J, Chen B, King EM, Borodovsky A, et al. Itraconazole and arsenic trioxide inhibit Hedgehog pathway activation and tumor growth associated with acquired resistance to smoothened antagonists. Cancer Cell. 2013; 23:23–34. [PubMed: 23291299]

Kimura H, Ng JM, Curran T. Transient inhibition of the Hedgehog pathway in young mice causes permanent defects in bone structure. Cancer Cell. 2008; 13:249–260. [PubMed: 18328428]

Koelsche C, Sahm F, Capper D, Reuss D, Sturm D, Jones DT, Kool M, Northcott PA, Wiestler B, Böhmer K, et al. Distribution of TERT promoter mutations in pediatric and adult tumors of the nervous system. Acta Neuropathol. 2013; 126:907–915. [PubMed: 24154961]

Kool M, Korshunov A, Remke M, Jones DT, Schlanstein M, Northcott PA, Cho YJ, Koster J, Schouten-van Meeteren A, van Vuurden D, et al. Molecular subgroups of medulloblastoma: an international meta-analysis of transcriptome, genetic aberrations, and clinical data of WNT, SHH, Group 3, and Group 4 medulloblastomas. Acta Neuropathol. 2012; 123:473–484. [PubMed: 22358457]

Korshunov A, Remke M, Kool M, Hielscher T, Northcott PA, Williamson D, Pfaff E, Witt H, Jones DT, Ryzhova M, et al. Biological and clinical heterogeneity of MYCN-amplified medulloblastoma. Acta Neuropathol. 2012; 123:515–527. [PubMed: 22160402]

Lee Y, Kawagoe R, Sasai K, Li Y, Russell HR, Curran T, McKinnon PJ. Loss of suppressor-of-fused function promotes tumorigenesis. Oncogene. 2007; 26:6442–6447. [PubMed: 17452975]

Lin TL, Matsui W. Hedgehog pathway as a drug target: Smoothened inhibitors in development. OncoTargets and therapy. 2012; 5:47–58. [PubMed: 22500124]

Louis DN, Ohgaki H, Wiestler OD, Cavenee WK, Burger PC, Jouvet A, Scheithauer BW, Kleihues P. The 2007 WHO classification of tumours of the central nervous system. Acta Neuropathol. 2007; 114:97–109. [PubMed: 17618441]

Low JA, de Sauvage FJ. Clinical experience with Hedgehog pathway inhibitors. J Clin Oncol. 2010; 28:5321–5326. [PubMed: 21041712]

Metcalfe C, Alicke B, Crow A, Lamoureux M, Dijkgraaf GJ, Peale F, Gould SE, de Sauvage FJ. PTEN loss mitigates the response of medulloblastoma to Hedgehog pathway inhibition. Cancer Res. 2013; 73:7034–7042. [PubMed: 24154871]

Milenkovic L, Scott MP. Not lost in space: trafficking in the hedgehog signaling pathway. Sci Signal. 2010; 3:pe14. [PubMed: 20388915]

Ng JM, Curran T. The Hedgehog's tale: developing strategies for targeting cancer. Nat Rev Cancer. 2011; 11:493–501. [PubMed: 21614026]

Northcott PA, Hielscher T, Dubuc A, Mack S, Shih D, Remke M, Al-Halabi H, Albrecht S, Jabado N, Eberhart CG, et al. Pediatric and adult sonic hedgehog medulloblastomas are clinically and molecularly distinct. Acta Neuropathol. 2011a; 122:231–240. [PubMed: 21681522]

Northcott PA, Korshunov A, Witt H, Hielscher T, Eberhart CG, Mack S, Bouffet E, Clifford SC, Hawkins CE, French P, et al. Medulloblastoma comprises four distinct molecular variants. J Clin Oncol. 2011b; 29:1408–1414. [PubMed: 20823417]

Northcott PA, Jones DT, Kool M, Robinson GW, Gilbertson RJ, Cho YJ, Pomeroy SL, Korshunov A, Lichter P, Taylor MD, Pfister SM. Medulloblastomics: the end of the beginning. Nat Rev Cancer. 2012a; 12:818–834. [PubMed: 23175120]

Northcott PA, Shih DJ, Peacock J, Garzia L, Morrissy AS, Zichner T, Stütz AM, Korshunov A, Reimand J, Schumacher SE, et al. Subgroup-specific structural variation across 1,000 medulloblastoma genomes. Nature. 2012b; 488:49–56. [PubMed: 22832581]

Padovani L, Sunyach MP, Perol D, Mercier C, Alapetite C, Haie-Meder C, Hoffstetter S, Muracciole X, Kerr C, Wagner JP, et al. Common strategy for adult and pediatric medulloblastoma: a multicenter series of 253 adults. Int J Radiat Oncol Biol Phys. 2007; 68:433–440. [PubMed: 17498567]

Parsons DW, Li M, Zhang X, Jones S, Leary RJ, Lin JC, Boca SM, Carter H, Samayoa J, Bettegowda C, et al. The genetic landscape of the childhood cancer medulloblastoma. Science. 2011; 331:435–439. [PubMed: 21163964]

Pugh TJ, Weeraratne SD, Archer TC, Pomeranz Krummel DA, Auclair D, Bochicchio J, Carneiro MO, Carter SL, Cibulskis K, Erlich RL, et al. Medulloblastoma exome sequencing uncovers subtype-specific somatic mutations. Nature. 2012; 488:106–110. [PubMed: 22820256]

Rausch T, Jones DTW, Zapatka M, Stütz AM, Zichner T, Weischenfeldt J, Jäger N, Remke M, Shih D, Northcott PA, et al. Genome sequencing of pediatric medulloblastoma links catastrophic DNA rearrangements with TP53 mutations. Cell. 2012; 148:59–71. [PubMed: 22265402]

Remke M, Ramaswamy V, Peacock J, Shih DJ, Koelsche C, Northcott PA, Hill N, Cavalli FM, Kool M, Wang X, et al. TERT promoter mutations are highly recurrent in SHH subgroup medulloblastoma. Acta Neuropathol. 2013; 126:917–929. [PubMed: 24174164]

Robinson G, Parker M, Kranenburg TA, Lu C, Chen X, Ding L, Phoenix TN, Hedlund E, Wei L, Zhu X, et al. Novel mutations target distinct subgroups of medulloblastoma. Nature. 2012; 488:43–48. [PubMed: 22722829]

Rudin CM, Hann CL, Laterra J, Yauch RL, Callahan CA, Fu L, Holcomb T, Stinson J, Gould SE, Coleman B, et al. Treatment of medulloblastoma with hedgehog pathway inhibitor GDC-0449. N Engl J Med. 2009; 361:1173–1178. [PubMed: 19726761]

Ryan SL, Schwalbe EC, Cole M, Lu Y, Lusher ME, Megahed H, O'Toole K, Nicholson SL, Bognar L, Garami M, et al. MYC family amplification and clinical risk-factors interact to predict an extremely poor prognosis in childhood medulloblastoma. Acta Neuropathol. 2012; 123:501–513. [PubMed: 22139329]

Shu Q, Wong KK, Su JM, Adesina AM, Yu LT, Tsang YT, Antalffy BC, Baxter P, Perlaky L, Yang J, et al. Direct orthotopic transplantation of fresh surgical specimen preserves CD133+ tumor cells in clinically relevant mouse models of medulloblastoma and glioma. Stem Cells. 2008; 26:1414–1424. [PubMed: 18403755]

Spreafico F, Massimino M, Gandola L, Cefalo G, Mazza E, Landonio G, Pignoli E, Poggi G, Terenziani M, Pedrazzoli P, et al. Survival of adults treated for medulloblastoma using paediatric protocols. Eur J Cancer. 2005; 41:1304–1310. [PubMed: 15869875]

Taylor MD, Northcott PA, Korshunov A, Remke M, Cho YJ, Clifford SC, Eberhart CG, Parsons DW, Rutkowski S, Gajjar A, et al. Molecular subgroups of medulloblastoma: the current consensus. Acta Neuropathol. 2012; 123:465–472. [PubMed: 22134537]

Wang Y, Ding Q, Yen CJ, Xia W, Izzo JG, Lang JY, Li CW, Hsu JL, Miller SA, Wang X, et al. The crosstalk of mTOR/S6K1 and Hedgehog pathways. Cancer Cell. 2012; 21:374–387. [PubMed: 22439934]

Welch JS, Ley TJ, Link DC, Miller CA, Larson DE, Koboldt DC, Wartman LD, Lamprecht TL, Liu F, Xia J, et al. The origin and evolution of mutations in acute myeloid leukemia. Cell. 2012; 150:264–278. [PubMed: 22817890]

Yauch RL, Dijkgraaf GJ, Alicke B, Januario T, Ahn CP, Holcomb T, Pujara K, Stinson J, Callahan CA, Tang T, et al. Smoothened mutation confers resistance to a Hedgehog pathway inhibitor in medulloblastoma. Science. 2009; 326:572–574. [PubMed: 19726788]

Yeh-Nayre LA, Malicki DM, Vinocur DN, Crawford JR. Medulloblastoma with excessive nodularity: radiographic features and pathologic correlate. Case reports in radiology. 2012; 2012:310359. [PubMed: 23133782]

Zhao X, Liu Z, Yu L, Zhang Y, Baxter P, Voicu H, Gurusiddappa S, Luan J, Su JM, Leung HC, Li XN. Global gene expression profiling confirms the molecular fidelity of primary tumor-based orthotopic xenograft mouse models of medulloblastoma. Neuro-oncol. 2012; 14:574–583. [PubMed: 22459127]

Zhukova N, Ramaswamy V, Remke M, Pfaff E, Shih DJ, Martin DC, Castelo-Branco P, Baskin B, Ray PN, Bouffet E, et al. Subgroup-specific prognostic implications of TP53 mutation in medulloblastoma. J Clin Oncol. 2013; 31:2927–2935. [PubMed: 23835706]

Significance

Our data show that most adults, but only half of the pediatric patients, with SHH-MB will likely respond to SMO inhibition as predicted by molecular analysis of the primary tumor and tested in the SHH xenografts, demonstrating that the next generation of SMO inhibitor trials should be based on these predictive biomarkers. Recurrent mutations in additional pathways suggest rational combination therapies including epigenetic modifiers and PI3K/AKT inhibitors, especially in adults. We also show that tumor predisposition (Gorlin syndrome and Li-Fraumeni syndrome) is highly prevalent in patients with SHH-MB. Each patient with SHH-MB, especially those 4–17 years old with LCA histology, should be tested for germline *TP53* mutations. Separate LFS-MB trials should be considered, sparing radiotherapy and excluding alkylating drugs.

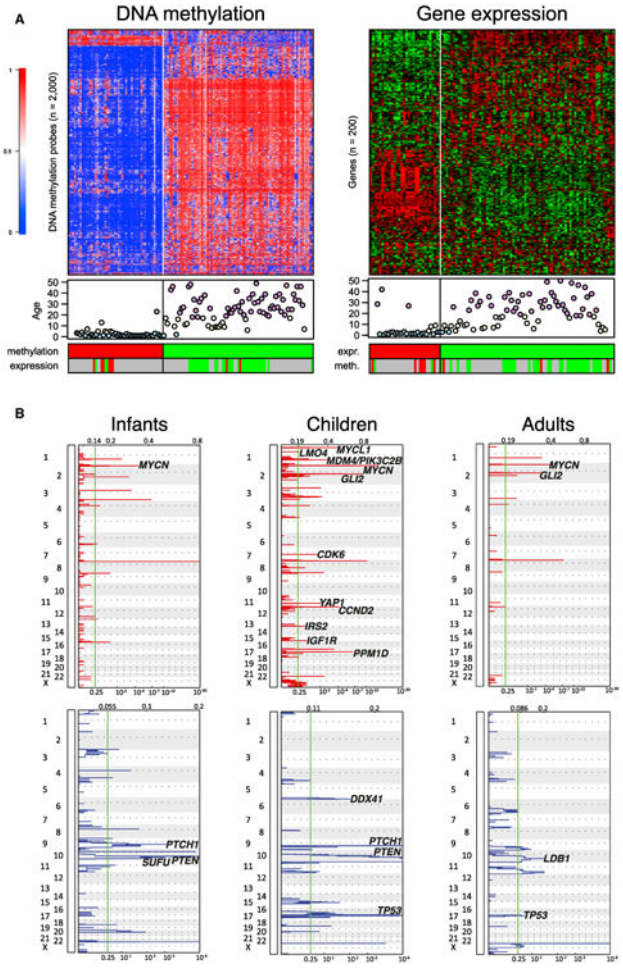

Figure 1. Genetic and Epigenetic Differences between SHH-MBs from Infants, Children, and Adults

(A) Cluster analysis of DNA methylation and gene expression data of SHH-MB. Both methylation profiling (left; n = 129) and gene expression profiling (right; n = 103) reveal two SHH-MB subgroups identified by unsupervised *k*-means consensus clustering. Each row represents a methylation probe/expression probeset, each column represents a sample. The level of DNA methylation (b value) is represented with a color scale as depicted. For each sample patient age (blue, infants; yellow, children; and pink, adults) and clustering according to expression data or methylation data (when available) is shown. Grey indicates that no data were available.

(B) GISTIC2 significance plots of amplifications (red) and deletions (blue) observed in SHH-MB infants, children, and adults. Candidate genes mapping significant regions have been indicated.

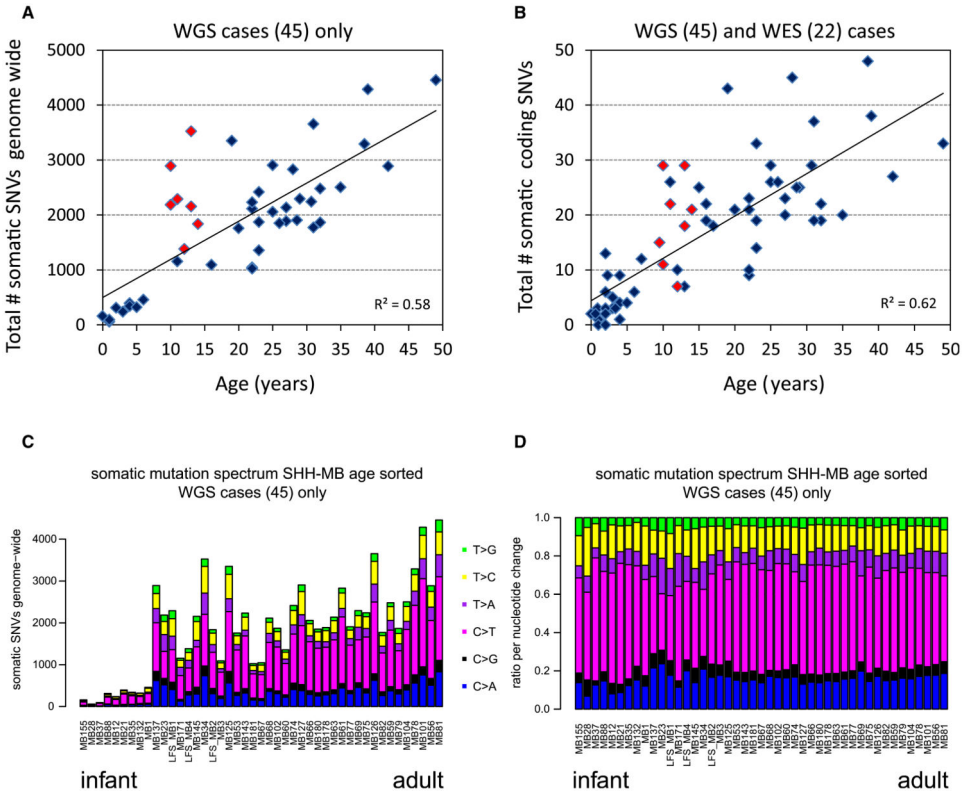

Figure 2. Number and Type of Somatic Mutations in Medulloblastoma Tumors in Relation to the Age of the Patient

(A) Total number of somatic mutations genome wide correlates with age of the patient. Plotted are the total number of somatic SNVs identified genome wide versus age of the patient for all cases for which we performed whole genome sequencing (WGS; n = 45). Red indicates patients harboring a *TP53* mutation.

(B) Same as in (A), but only the total number of coding SNVs is plotted versus age for all cases for which we performed either whole genome or whole exome sequencing (WGS and WES, n = 67).

(C) Mutation signatures. Plotted are the total numbers of somatic mutations genome wide sorted by age of the patient. Coloring of bars represents the ratio of the six possible nucleotide changes (C > A, C > G, C > T, T > A, T > C, and T > G) for each sample.

(D) Normalized mutation signatures sorted by age.

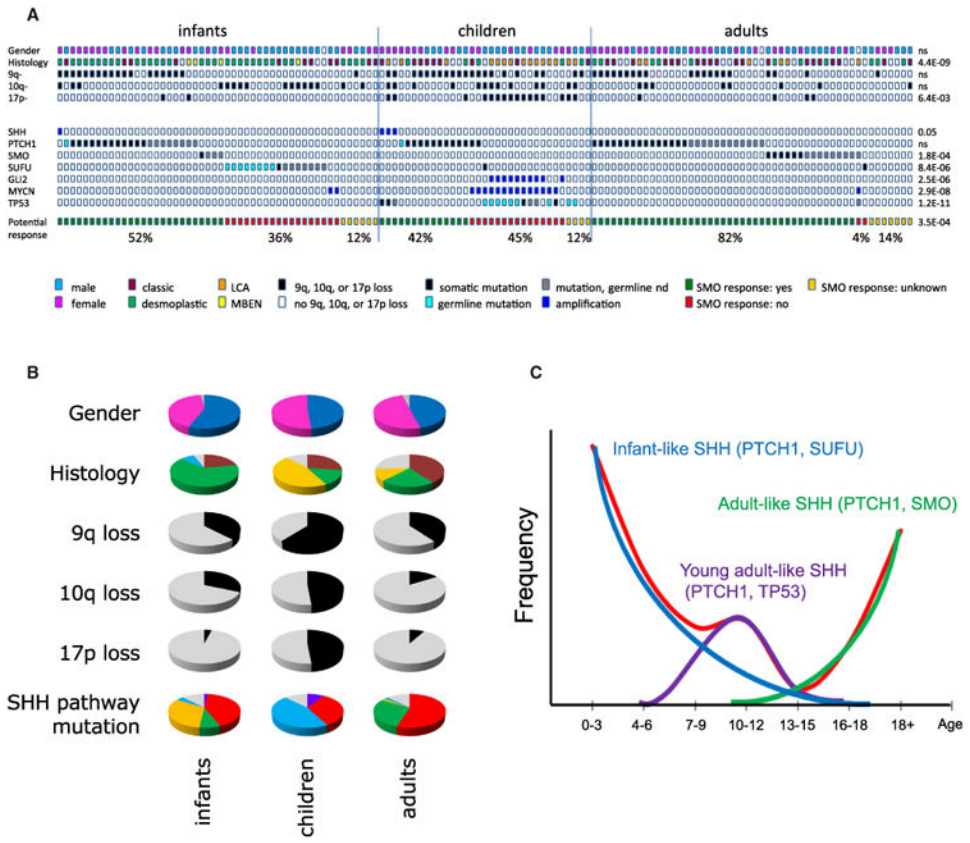

Figure 3. Genetic and Histological Differences between SHH-MBs from Infants, Children, and Adults

(A) SHH pathway mutations, gender, histology and 9q/10q/17p aberrations in all sequenced 133 SHH-MB. Cases have been split up in infants, children and adults, and are sorted based on type of mutation in the SHH-pathway. Potential response to SMO inhibition: cases with *SHH* amplifications, *PTCH1* mutations, or *SMO* mutations will likely respond to SMO inhibition (indicated in green). Cases with *SUFU* mutations or *MYCN* or *GLI2* amplifications will likely not respond to SMO inhibition (indicated in red). In cases for which no mutations in the SHH pathway were detected, it is not clear whether they will respond to SMO inhibitors (indicated in yellow). Percentages indicate fraction of infants, children, or adults, respectively, of each category. p Values indicate whether distributions are significantly different among infants, children, and adults.

(B) Pie charts showing in infants, children, and adults with SHH the distribution of gender (male, blue; female, pink; unknown, gray), histology (classic, dark red; nodular/desmoplastic, green; large cell/anaplastic LCA, orange; MBEN, yellow; and unknown, gray), 9q loss (yes, black; no, gray), 10q loss (yes, black; no, gray), 17p loss (yes, black; no, gray), and type of SHH pathway mutation (*SHH* amp, purple; *PTCH1* mut, red; *SMO* mut, green; *SUFU* mut, orange; *GLI2*/*MYCN* amp, blue; and unknown, gray).

(C) Trimodal age distribution of patients with SHH-MB. Red line indicates age distribution of all patients with SHH-MB. Three subgroups make up this age distribution: young children with *PTCH1* and *SUFU* mutations (blue line), older children with *PTCH1* and

TP53 mutations (purple line), and adults who mostly have *PTCH1* or *SMO* mutations (green line).

See also Figure S1.

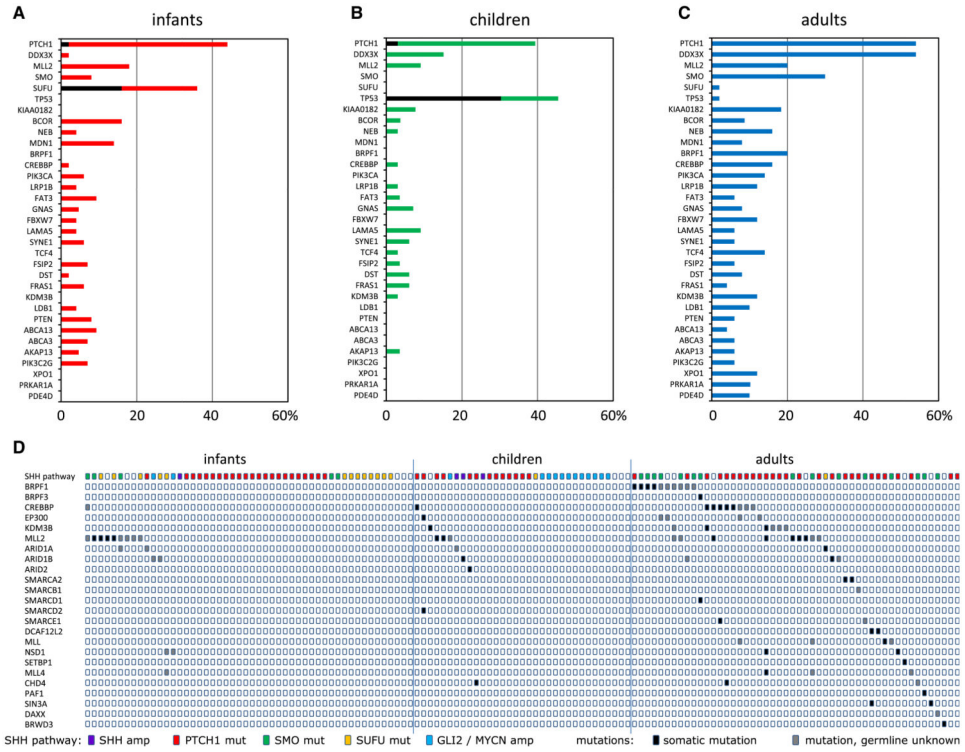

Figure 4. Most Frequently Mutated Genes in SHH-MB and the Mutual Exclusivity of Mutations in Chromatin Modifier Genes

(A–C) Mutation frequencies of 33 genes that are mutated either in ≥5% of all SHH-MB cases or in ≥10% of SHH-MB cases in one of the age categories. Mutation frequencies for these 33 genes are shown in infants (A), children (B), and adults (C). Black indicates the fraction of mutations that is found in the germline.

(D) Mutations in chromatin modifiers in infants, children, and adults with SHH-MB. The top line shows the mutations in the SHH pathway for each case.

See also Figure S2.

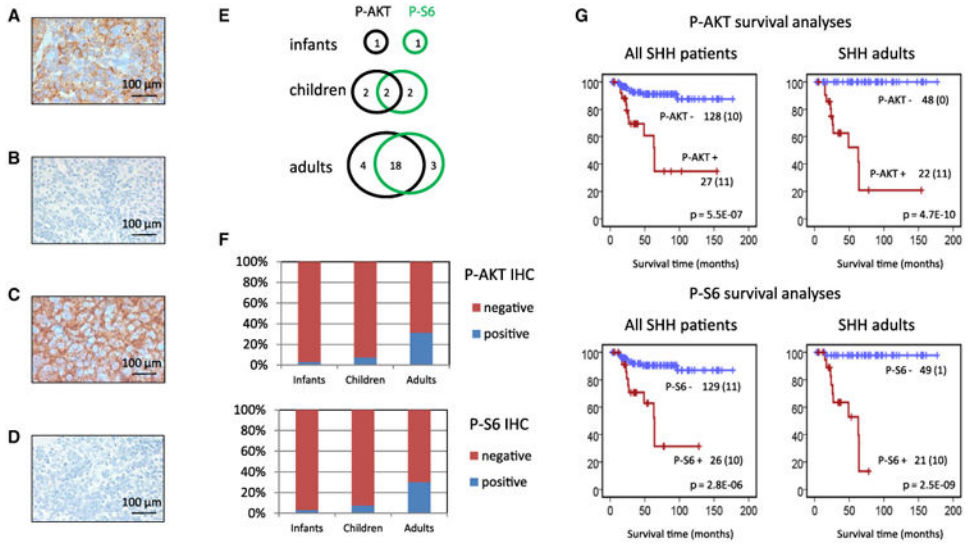

Figure 5. Immunohistochemical Staining of MB Tissue Arrays for p-AKT and p-S6

(A) Example of positive p-AKT MB.

(B) Example of negative p-AKT MB.

(C) Example of positive p-S6 MB.

(D) Example of negative p-S6 MB.

(E) Overlap in staining results between p-AKT and p-S6.

(F) Frequencies of p-AKT and p-S6 staining in infants, children, and adults.

(G) Survival analysis for p-AKT and p-S6 in all SHH patients and in adults only. Numbers on the y-axis indicate the fraction of surviving patients. Numbers on the x-axis indicate the follow-up time in months. The number of patients per group is indicated next to the graphs plus the number of events within that group (between brackets). For infants and children, the number of patients staining positive was too low to draw conclusions from separate survival analyses.

A

case #	MB subgroup	patient age	gender	tumor histology	mutation
DMB-012	SHH	3	female	desmoplastic	*PTCH1* (4 bp del, hemizygous)
RCMB-018	SHH	7	male	anaplastic	*TP53* (R175H, hemizygous) *MYCN* amplification
RCMB-025	SHH	0	female	MBEN	*SUFU* deletion (heterozygous)

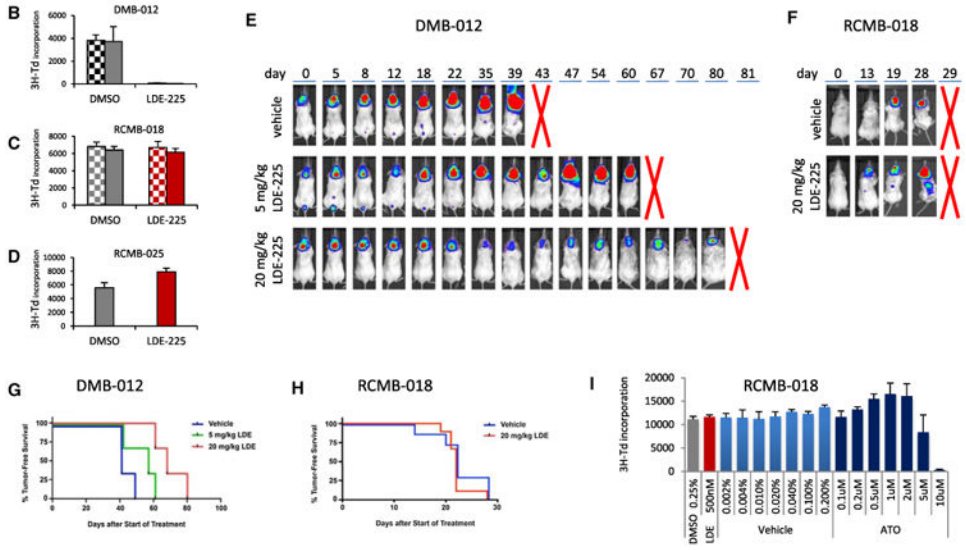

Figure 6. SMO Antagonists Do Not Suppress Proliferation of All SHH-Associated MB Tumors

(A) Characteristics of SHH-MB models treated with LDE225.

(B–D) Cells from patient-derived xenografts of SHH-associated MB were treated with DMSO (0.05% [hatched bars] or 0.25% [solid bars]) or LDE-225 (100 [hatched bars] or 500 nM [solid bars]). Cells were pulsed with [methyl-^{3}H]thymidine (^{3}H-Td) after 48 hr and harvested for analysis of ^{3}H-Td incorporation at 66 hr. In DMB-012 (B), LDE-225 significantly inhibited ^{3}H incorporation compared to DMSO control ($p < 0.01$ based on paired two-tailed t test). In RCMB-018 (C) and RCMB-025 (D), LDE-225 did not significantly inhibit ^{3}H incorporation ($p > 0.5$ and $p > 0.1$, respectively). Data represent means of triplicate samples ± SD.

(E and F) Cells from MB xenograft DMB-012 (E) or RCMB-018 (F) were infected with luciferase virus and transplanted into NSG mice. Bioluminescence images were taken pretreatment (day 0) and at different time points after daily treatment with vehicle or SHH antagonist (LDE-225, 5 or 20 mg/kg/day). Five mice per group were used. Representative examples from each group are shown. Other examples are shown in Figure S3. A red cross indicates when mice were sacrificed.

(G and H) Kaplan-Meier survival plots for the mice harboring DMB-012 tumors (G) or RCMB-018 tumors (H) and treated with vehicle or LDE-225.

(I) RCMB-018 cells were treated with DMSO (0.25%; gray bar), LDE-225 (500 nM; red bar), vehicle (PBS + 0.01 N NaOH; light blue bars), or increasing concentrations of ATO (dark blue bars). Cells were pulsed with [methyl-^{3}H] thymidine (^{3}H-Td) after 48 hr and harvested for analysis of ^{3}H-Td incorporation at 66 hr. LDE-225 did not inhibit ^{3}H incorporation compared to DMSO control, but ATO did at 5 and 10 μM concentrations. Data represent means of triplicate samples ± SD.

See also Figure S3.

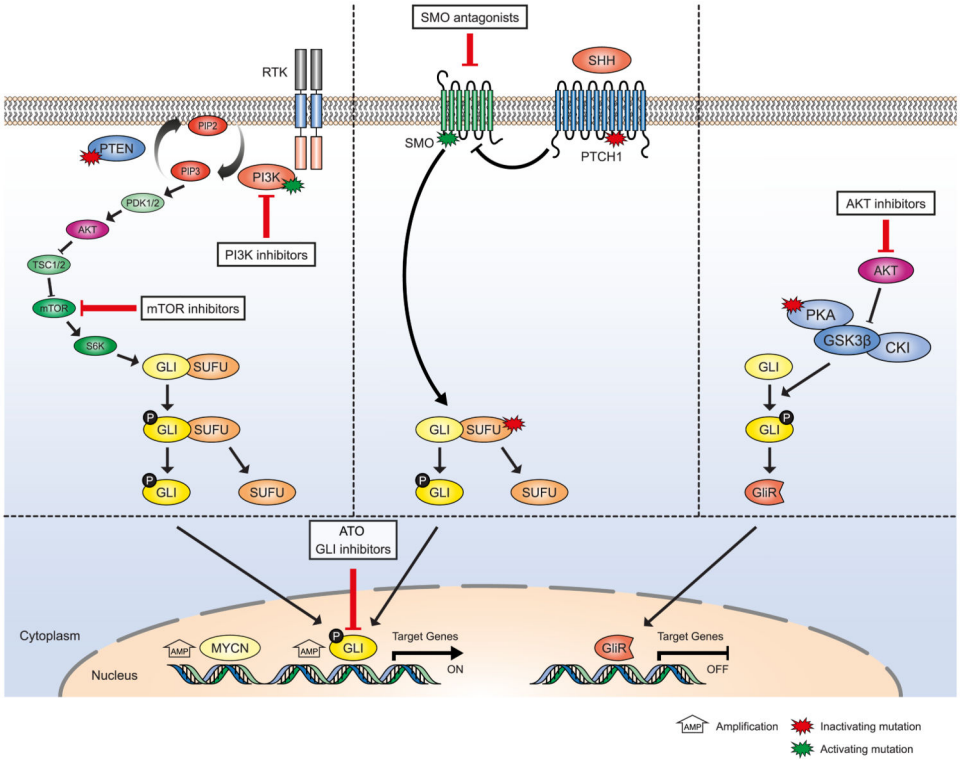

Figure 7. Schematic Overview of SHH-, PI3K/AKT/mTOR-, and PKA Pathways and How They Interact

Genes that were found in the genomic analyses of SHH-MBs to harbor activating mutations (green stars), inactivating mutations (red stars), or were found to be amplified (*MYCN* and *GLI*) are indicated. All these mutations lead to activation of GLI proteins and their downstream pathways. Options for targeted treatment are indicated. Patients harboring mutations in either *PTCH1* or *SMO* should be responsive to SMO inhibitors, whereas patients harboring mutations more downstream in the SHH pathway (*SUFU*, *MYCN*, and *GLI*) or in the PI3K/AKT/mTOR and/or PKA-pathways may be treated using arsenic trioxide (ATO) or other more specific GLI-inhibitors or PI3K/AKT/mTOR inhibitors.

Table 1

SHH-MB Patient Cohorts

Cohort	Number of Patients
Whole genome sequencing[a]	n = 45
Infants[b]	5
Children[c]	13
Adults[d]	27
Whole exome sequencing[a]	n = 22
Infants	13
Children	9
Adults	0
Targeted sequencing 2734 genes[a] 12	n = 12
Infants	7
Children	5
Adults	0
Targeted sequencing 400 genes[e]	n = 54
Infants	25
Children	6
Adults	23
Immunohistochemistry	n = 155
Infants	31
Children	54
Adults	70

See also Tables S1, S2, S3, and S4.

[a] Tumor-normal pairs were sequenced.

[b] Infants: 0–3 years of age.

[c] Children: 4–17 years of age.

[d] Adults: ≥ 18 years of age.

[e] Only tumors were sequenced.